

Core emission in classical conal double pulsars

Stephanie A. E. Young[★] and Joanna M. Rankin[★]

Physics Department, University of Vermont, Burlington, VT 05405, USA

Accepted 2012 April 6. Received 2012 March 30; in original form 2011 August 30

ABSTRACT

A focus on single-pulse methods has identified what appears to be core emission in pulsars B0525+21, B0301+19 and B1133+16. Such core emission has been suspected in several ‘classical’ double conal pulsars; however, previous methods of analysis have restricted our ability to look further into this possibility. While average profiles of pulsars inform about the typical behaviours of these stars, single-pulse observations shed light on the atypical behaviours and weak features of a pulsar’s emission. Emission in the ‘intrapulse region’ is not detectable in the average profiles but becomes clear in low-intensity and single-pulse observations. Through a process of suppressing the outer conal emission and averaging non-consecutive pulses that exhibit peaks in a central search region, reliable partial profiles of these putative core features have been obtained. In each case, the widths of the central features squared well with the expected polar cap geometry, further strengthening their identification with core emission components.

Key words: pulsars: general – pulsars: individual: B0301+19 – pulsars: individual: B0525+21 – pulsars: individual: B1133+16.

1 INTRODUCTION

The small population of radio pulsars with wide double profiles has exerted a strong influence on conceptions of pulsar emission. Their ‘S’-shaped polarization position angle (PPA) traverses, broadening with wavelength (i.e. ‘radius-to-frequency mapping’), steep outer and shallow inner edges and edge depolarization (e.g. see Mitra & Rankin 2002; Rankin & Ramachandran 2003; Hankins & Rankin 2010) have gained them special notice since shortly after the pulsar discovery. This conal double configuration lies at the very centre of geometrical classification efforts and their empirical interpretation (Radhakrishnan & Cooke 1969; Komesaroff 1970; Backer 1975; Rankin 1983, hereafter ET I; Lyne & Manchester 1988) – and this was the only type of emissivity that the Ruderman & Sutherland (1975) theory attempted to explain physically. Following this long record of study and interpretation, we refer to such pulsars as exhibiting ‘classic’ double profile forms.

We now know that pulsar emission profiles are generally more complex than these ‘classic’ double forms would indicate, showing consistent geometrical evidence of two concentric hollow conical emission regions as well as a central core beam (e.g. Rankin 1993a, hereafter ET VIa; Rankin 1993b, hereafter ET VIb; Mitra & Rankin 2011). In particular, the ‘intrapulse’ region falling in between the leading and trailing components of such ‘classic’ double profiles has long raised questions: the emission in this area seems not to be comprised entirely of the ‘tails’ of the two bright conal components, nor

does it ever seem to form a ‘component’ in its own right. Most such interpretations have been based entirely on average profile methods. In a few cases, fluctuation spectral techniques have identified distinct long-period modulation features in this region, suggesting that the ‘intrapulse’ emission was not conal and thus possibly core in character (see Rankin 1986, and the references therein); however, more recent studies have tended to associate these features with periodic nulling (Herfindal & Rankin 2007, 2009).

Here we undertake a full investigation of the ‘intrapulse’ emission in the few bright stars with ‘classic’ conal double (D) profiles visible with the Arecibo telescope. We have access to sensitive pulse sequence (PS) polarimetry in two different bands; therefore, we can much more fully investigate the single-pulse properties of this emission. Overall, we find evidence for core emission in the ‘intrapulse’ region – i.e. core emission that is not necessarily weak but so sporadic that it contributes little to the total average profiles. In Section 2 we describe our observations, and in Section 3 we present the results of our analyses. Section 4 gives a summary and discussion of our results.

2 OBSERVATIONS

The observations were carried out using the 305-m Arecibo Telescope in Puerto Rico. All of the observations used the upgraded instrument with its Gregorian feed system, 327-MHz (*P*-band) or 1100–1700 MHz (*L*-band) receivers, and Wideband Arecibo Pulsar Processors. The auto- and cross-correlations (ACFs and CCFs) of the channel voltages produced by receivers connected to orthogonal linearly (circularly, after 2004 October 11 at *P* band) polarized feeds

[★]E-mail: stephanie.young@uvm.edu (SAEY); joanna.rankin@uvm.edu (JMR)

Table 1. Observational parameters.

Pulsar	RF (MHz)	Date (m/d/yr)	Length (pulses)	Res. (°)
B0301+19	1420	07/17/2003	2163	0.27
	1420	08/03/2003	1297	0.27
	327	01/08/2005	1729	0.19
B0525+21	1420	10/01/2009	1441	0.20
	327	10/4/2003	636	0.35
	327	09/30/2009	1505	0.36
B1133+16	1400	08/03/2003	1010	0.31
	1520	08/03/2003	1010	0.31
	327	05/02/2005	1342	0.39

were three-level sampled. Upon Fourier transforming, some 64 or more channels were synthesized across the passbands with about a millisecond sampling time. At P band, 25-MHz bands were used prior to 2009 and 50 MHz thereafter. Three bands centred at 1170, 1420 and 1520 MHz were available at L band, and the lower three were often free enough of radio-frequency interference (RFI) such that they could be added together to give 300-MHz bandwidth at nominally 1400 MHz. Each of the Stokes parameters was corrected for interstellar Faraday rotation, various instrumental polarization effects and dispersion. The date, resolution and the length of the observations are listed in Table 1.

3 ANALYSES

During the course of some earlier investigations we had noted occasional strong subpulses near the profile centres of bright pulsars well known for their conal double profiles and ‘S’-shaped PPA traverses. In that these subpulses almost always occurred singly, they were readily dismissed as probably part of a ‘tail’ distribution associated with the two bright conal components. However, a possible ‘core flare’ in a short early observation of pulsar B0525+21 kindled a more serious interest: here any core activity seemed doubly unlikely, first because the star had a ‘classic’ conal double profile and second because of its long 3.7-s rotation period.

Fig. 1 gives a 200-pulse polarization display of this early observation of pulsar B0525+21, and the putative ‘core flare’ can be seen near the bottom of the left-hand (total power) column during pulses 414–435. No other such emission structure is seen in the remainder of the short 636-pulse observation, though emission is seen in the centre of the profile, sometimes in the form of weak subpulses that peak in this region, but often also as emission that ‘spills over’ from the bright conal components. Note also that the polarization characteristics of the emission change little during the ‘core flare’: the PPA and circular polarization imperceptibly; the only clear change is in the fractional linear where the centre of the profile appears somewhat more depolarized as if the ‘flare’ represented secondary polarization-mode power.

We have waited some time to undertake this study because we wanted to conduct much longer observations of B0525+21, and these became possible only towards the end of 2009. In the meantime we encountered preliminary evidence that similar effects might occur in other ‘classic’ conal double pulsars, and we present analyses below of both B0301+19 and B1133+16. Some work was also carried out on several weaker stars with prominent conal double profiles, but the lower signal-to-noise ratio (S/N) prevented our obtaining clear results.

Fig. 2 displays a total average profile as well as a low-intensity partial profile, both of B0525+21 at 327 MHz. The latter is com-

prised of 370 pulses with intensities ranging from 0.3 to 0.9 (I). Clearly, these pulses are not usually consecutive. The small new peak in the centre of the partial profile occurs at just the position where possible core-emission components sometimes occur. This feature closely coincides with the S-shaped swing of the PPA, whose steepest gradient falls at about 0° longitude. In fact, the somewhat asymmetric feature peaks near $+1^\circ$, and note that there is a weak inflection in the total average profile at just this point. Possibly such features have been missed because they were ‘swamped’ by other emission in this region. The observed steep PPA traverse through nearly 180° indicates that our sight-line passes directly across the centre of the emission cone, close to the magnetic axis along which core beams are thought to be emitted; indeed, modelling suggests that the sight-line impact angle β is only 0.6 (ET VIa; ET VIb). Note that the partial profile, in I and L , gives a clear indication of inner and outer conal component structure as well.

3.1 Are ‘intra-subpulses’ of the core type?

Mere identification of a population of subpulses in the intrapulse region surely does not show that they represent core emission. In order to make any such interpretation, we need to show that the population is confined to a *narrow* central region – thus is *not* ‘spillover’ from the intense adjacent outer conal emission. Core widths reflect the angular extent of a pulsar’s polar cap, so we must show that the population has an aggregate partial profile width that reflects this origin. Further, core emission is usually broad band in nature; and it sometimes exhibits strong antisymmetric circular polarization.

Overall, if the weak ‘intra-subpulses’ we saw above in fact comprise a core emission feature, then we might expect them to exhibit peaks near the profile centre and aggregate to a distinct feature. Partial profiles are often computed using a criterion that the individual pulses have a peak in a certain range, but the method fails here to identify intrapulse peaks because the adjacent conal emission is usually dominant. Therefore, we developed a method to attenuate the conal emission. (a) we noted the relative height and extent of the intrapulse ‘bridge’ in the average profile and took this to estimate its relative intensity and width in individual pulses. (b) The individual pulse emission outside this range was attenuated to the ‘bridge’ level and then a search was made for a peak in the intrapulse region. (c) Individual pulses exhibiting a peak in this region were accrued to form a partial average profile. This method worked well on all three pulsars at both frequencies, although we found that the search range had to be restricted to avoid inner conal emission.

3.2 Pulsar B0525+21

In Fig. 3, we present the first results of our ‘outer conal suppression’ method, here also at 327 MHz, where the top-left panel shows the total profile and the bottom-left one the partial one. Note that the outer conal components have been effectively attenuated, leaving a central feature together with a pair of other features on its flanks. These latter we see as mere inflections in the total profile, but their position and symmetry here identify them as associated with inner cone emission. The displayed partial profile was computed using an attenuation level of 23 per cent (I) and a search width of ± 2.34 such that 80 pulses with qualifying central subpulse peaks were identified and averaged. Many trials were made with different attenuation levels and search widths, and virtually all showed a central feature of about the width seen. More outer cone suppression or broader

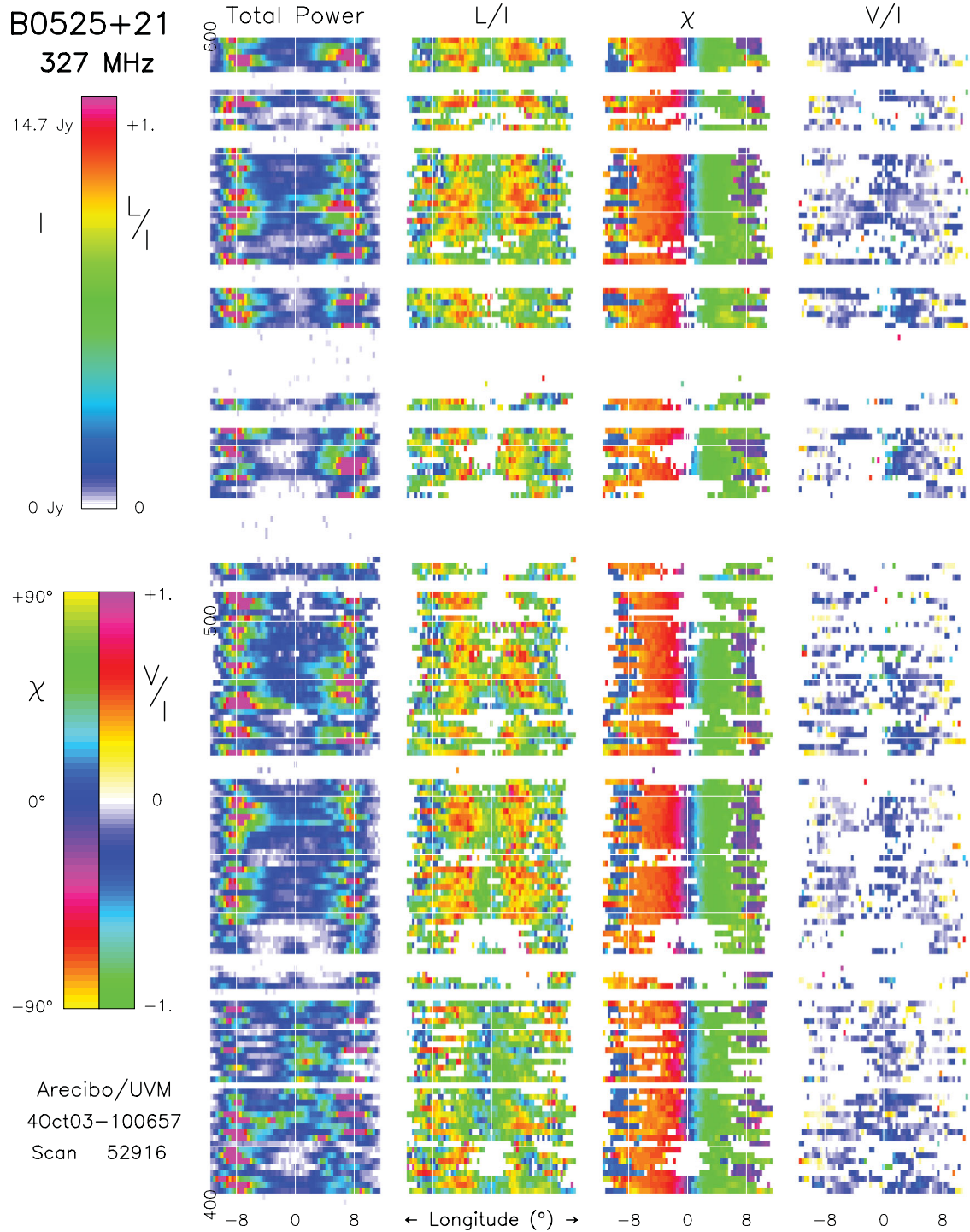


Figure 1. An unusual ‘core flare’ seen in the ‘classic’ conal double pulsar B0525+21 during pulses 414–435 at 327 MHz on 2003 October 4 (bottom of left-hand column). The 200-pulse polarization display shows this behaviour clearly: generally, bright emission is seen only in the leading and trailing conal components, not often in the central ‘intrapulse’ region of the profile, nor forming a distinct peak. No other such ‘flare’ was seen in the rest of this observation, but occasional weak subpulses are found near the centre of the profile (e.g. pulses 444 and 591). The total power I , fractional linear L/I , PPA χ and fractional circular polarization V/I are colour coded in each of four columns according to their respective scales at the left of the diagram. Note also that χ and V/I change hardly at all during the ‘flare’; rather the central region appears depolarized in the L/I column. Both the background noise and interference levels of this observation are exceptionally low, with the former disappearing into the lowest intensity white portion of the I colour scale.

searches for peaks favoured the inner conal subpulses, such that they quickly aggregated to overtake the central feature. Clearly, this central feature is not dissimilar to central emission seen in the ‘core flare’ or revealed through selection of a weaker population of

pulses, so it remains very possible that the central feature can justly be interpreted as core emission.

We have also searched for possible core-associated subpulses at 1400 MHz. The lower relative intrapulse power level at L band

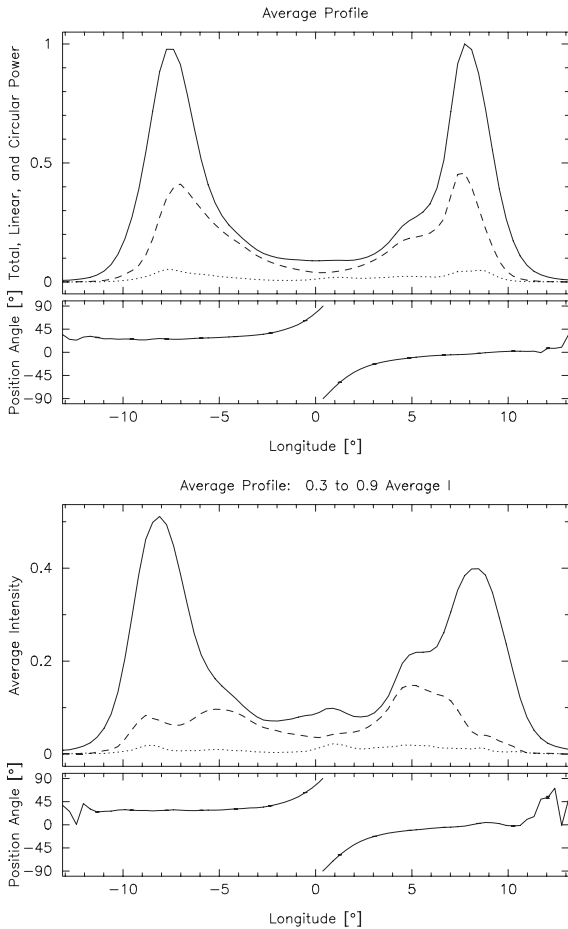


Figure 2. Total average profile of pulsar B0525+21 at 327 MHz (top) comprised of 1505 pulses together with a low-intensity partial profile (bottom) composed of 370 non-consecutive pulses having intensities falling between 0.3 and 0.9 (I). Note the emergence of a new profile feature near longitude 0° . Both panels display the total power, total linear polarization ($L = \sqrt{Q^2 + U^2}$; dashed) and circular polarization V (dotted) as well as (lower panel) the PPA [$=\frac{1}{2} \tan^{-1}(U/Q)$].

frustrated our attempts to identify weak central emission using the same method as in Fig. 2. Therefore, we invoked the above suppression method and the lower-right panel of Fig. 3 shows the resulting partial profile comprised of 51 qualifying pulses using an attenuation level of 23 percent (I) and a ± 2.46 search interval. This narrower search window reflects the star’s narrower profile at L band, its weaker ‘intrapulse bridge’, the more conflated structure of its profile components here and probably also the usually weaker relative intensity of core emission at higher frequencies.

Interestingly, we also analysed a display of this observation by eye and identified 39 individual pulses with peaks in the central $\pm 3^\circ$ region. The partial profile of those single pulses (not shown) exhibits a central peak with a half-power width of $3.5\text{--}4.0$ and falling close to the PPA steepest gradient point.

Thus, a reasonable estimate for the width of these putative core features in B0525+21 is between 3° and 4° longitude. In that core components seem to reflect the full angular width of the polar cap (Rankin 1990, hereafter ET IV), this value squares well with a polar cap diameter of 1.3 viewed at a magnetic colatitude α of 21° – i.e. 3.6 .

As for individual core ‘flares’, as seen in Fig. 1, similar flare-like activity was observed in the second P -band observation used in this

study. While a similar plot was not included here, other ‘core-flare’ sequences were observed and prompted us to use the later P -band observation in our low-intensity partial profile in Fig. 2. From this we may conclude that multiple core-flare events can be observed in longer observations and may give us insight into the inner workings of the core emission mechanisms we see in this pulsar.

3.3 Pulsar B0301+19

Fig. 4 displays the outer conal suppression partial profiles and their corresponding average profiles at both 327 and 1400 MHz – left and right, respectively. Here our effort was more difficult because the ‘intrapulse’ region often shows power that is clearly associated with the ‘tails’ of the leading and trailing conal components. None the less, at P band we see a strong central peak in intensity falling close to the PPA inflection point near 0° . This star’s sight-line traverse is the least central, so the suppression level was higher at 0.3 (I) and the search region a constricted ± 2.04 around the profile centre. At L band, a suppression level of 0.24 (I) was used together with a search region of ± 1.99 . These partial profiles include 130 and 21 pulses, respectively. The apparently larger core width at L band is doubtlessly misleading, owing to the difficulty of distinguishing here between the core and the obviously intruding inner conal sub-pulses such that few qualify. In fact, any wider intrapulse search region results in what appears to be a four-component partial profile. This ‘disappearance’ of the core feature is due to the relative weakness of the core compared to the inner conal components.

Additionally, a close visual study was made of the star’s subpulse patterns both at P and L bands, and a typical sequence of the latter is given in the left-hand panel of Fig. 5. Detailed examination of the single pulses showed a small population of moderately strong subpulses with peaks in the central $\pm 2^\circ$ region. An artificial PS of 39 such pulses, drawn from the longer of the two L -band observations, is shown in Fig. 6. This is usefully compared with the total profile in Fig. 4 (top-left panel), where the narrow spacing of the two outriding features suggests that the bright central subpulses are often accompanied by inner conal emission. A similar effort was made at 327 MHz where 93 pulses were identified with peaks in the central $\pm 3^\circ$ region. A partial profile of these pulses (not shown) exhibited the expected peak with a half-power width of about 3° and coincided with the steepest portion of the PPA traverse around $+1^\circ$ longitude. Further, this ‘core’ peak lagged the total profile centre by about half a degree, roughly what might be expected for the effects of aberration/retardation.

A study of this star at L band using single-pulse analysis also reveals emission in the centre of the profile, although here again we may expect that any core emission will be relatively weaker. Fig. 5 (left) displays a total power PS that illustrates the difficulties of analysis. Here, significant central emission often seems to persist for two to four pulses, but the longitude interval that can be clear of conal subpulses is little more than $\pm 2^\circ$ wide. Fig. 6 then shows some of the strongest examples of single pulses with central peaks assembled into an artificial 39-pulse PS display in the main panel and the corresponding partial average profile in its lower panel. Again, the triple character of this partial profile is fully expected as is the necessary dominance of the central component. What is significant is that the half-power width of the putative core is some 3.5 , well less than the width of the intrapulse region, and that the central peak lags the centre of conal components as in the P -band partial profile above.

Both our difficulties and results are more understandable in terms of the sight-line geometry of B0301+19. Its impact angle β of some

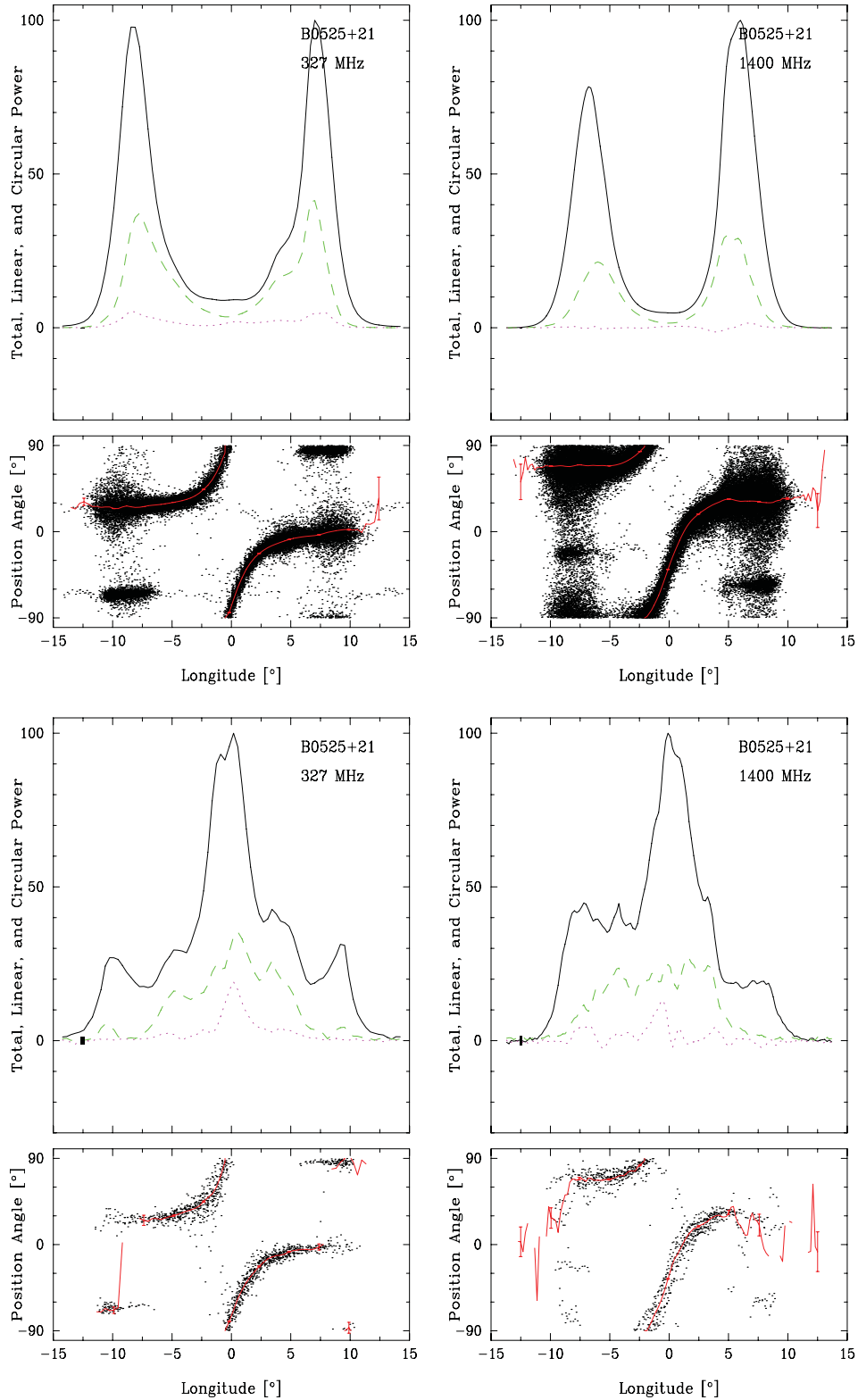


Figure 3. Total average profile (upper left) and suppressed outer conal partial profile (lower left) of B0525+21, both at 327 MHz. The latter was created using a suppression level of 0.23 (I) and an intrapulse search region of $\pm 2^\circ 34$. 1505 and 80 pulses were averaged, respectively. A similar pair of average (upper right) and partial (lower right) profiles correspond to B0525+21 at 1400 MHz. The partial profile entailed a conal suppression level of 0.23 (I) and a search region of $\pm 2^\circ 46$. 1441 and 51 pulses were averaged, respectively. Both partial profiles show significant emission in the intrapulse region near the steepest gradient point of the PPA traverse. At 327 MHz, inner conal components also clearly appear in addition to the putative core.

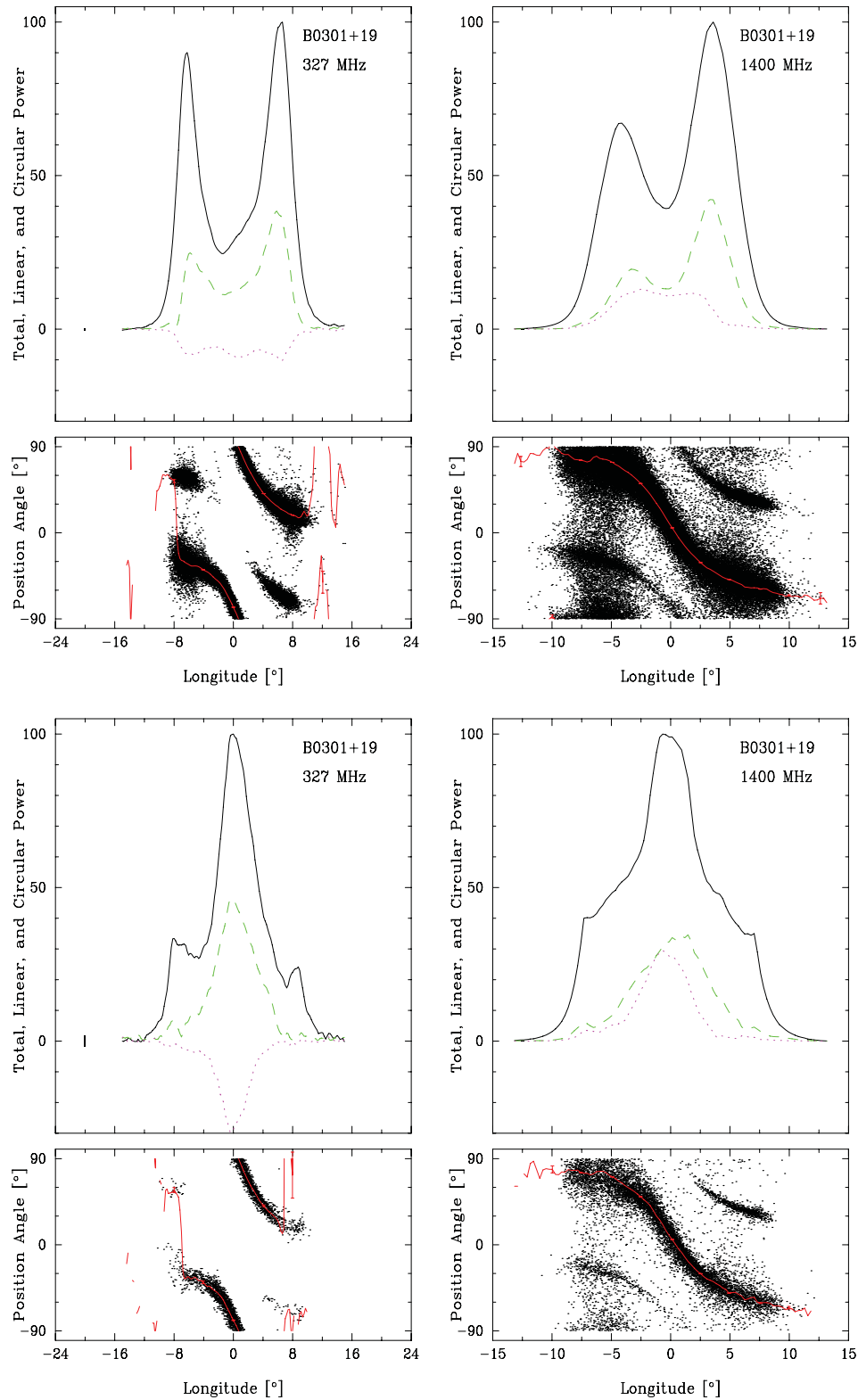


Figure 4. Total average (upper) and suppressed outer conal (lower) profiles of pulsar B0301+19 at both 327 MHz (left) and 1400 MHz (right) as in Fig. 3. At the lower frequency, the suppression level was 0.3 (I) and the intrapulse search region $\pm 2^{\circ}04$ wide, such that 1729 and 130 qualifying pulses were averaged, respectively. At 1400 MHz, the suppression level was 0.24 (I) and the search region width was $\pm 1^{\circ}99$, so 1297 and 211 pulses were averaged. Both lower plots show significant emission in the intrapulse region, although this region is so narrow at the higher frequency that some ‘spillover’ was unavoidable, probably contributing to the larger width here (see text).

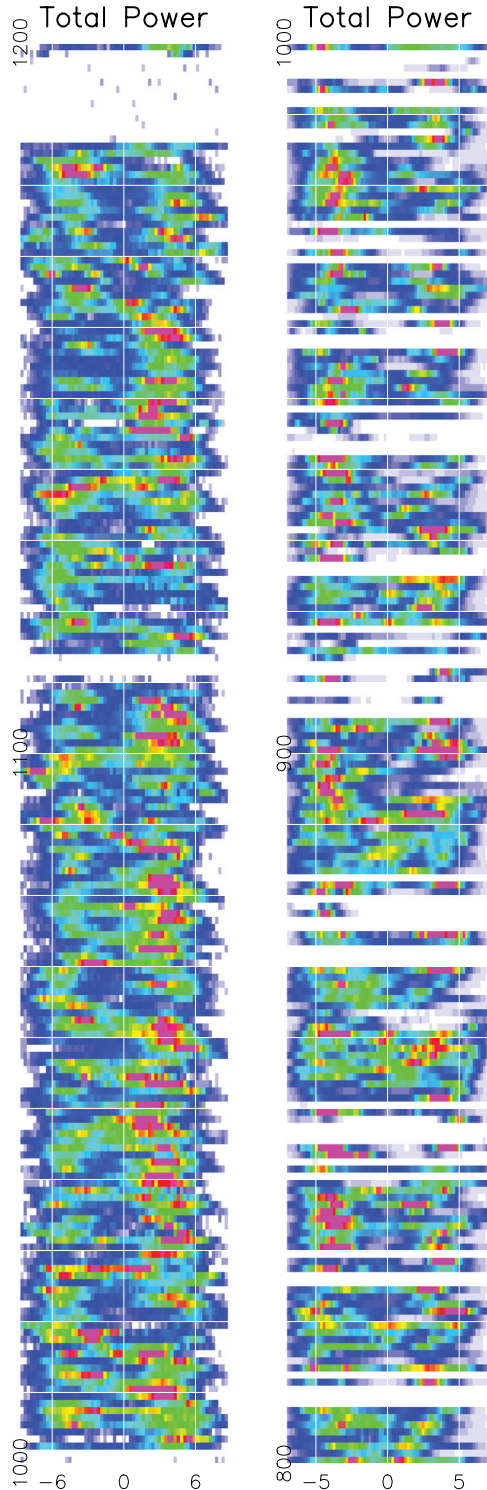


Figure 5. Colour intensity coded 200 PSs of B0301+19 (left at 1420 MHz) and B1133+16 (right at 327 MHz) showing relative scaling in the total power. Careful inspection of each image will show examples of subpulses that peak close to the centre of their respective profiles. Such activity is seen throughout our observations. The horizontal scale is in degrees of longitude.

1:7 together with the strong presence of inner-cone (in addition to the dominant outer-cone) emission results in a profile that is more closely spaced with less well-resolved peaks. Accordingly, its expected polar cap diameter of 2:1 is viewed at a magnetic latitude α

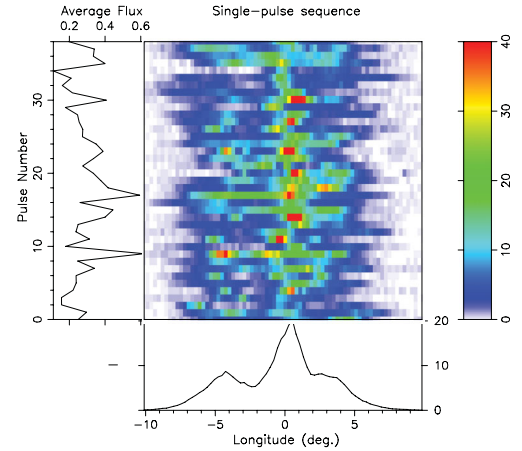


Figure 6. Pulsar B0301+19 at 1400 MHz: an artificially ordered, 39-pulse PS of single pulses with clear peaks in the central region, together with its partial average profile (lower panel).

of some 30° , implying a core width of some 4° in decent agreement with the rough measurements above.

3.4 Pulsar B1133+16

Fig. 7 presents another set of outer conal suppression plots at both 327 and 1520 MHz (left and right, respectively). Here again, the very shallow PPA traverse implies a poorly resolved profile with a high, narrow ‘intrapulse bridge’ region. For this pulsar at 327 MHz a suppression level of 0.2 (I) was used together with a mere $\pm 1:57$ search region, such that there are 180 qualifying pulses in the partial profile. At 1520 MHz an attenuation level of 0.3 (I), and a central region of $\pm 1:24$ was searched to identify the displayed 120-pulse partial profile. The expected strong central peaks fall close to the profile centre in both cases and have widths of some 3° – 4° .

As a check we also conducted visual analyses of the PSs, part of one of which is displayed in Fig. 5 (right-hand panel). The results of the 327-MHz effort is shown in Fig. 8, where a partial profile comprised of 26 pulses falling in a $\pm 2^\circ$ central region is displayed. The pulsar is so bright and the observation so sensitive that only a few pulses provide a high-quality partial average profile. Curiously, this profile exhibits two pairs of features in addition to the central one, corresponding almost certainly to emission from the inner cone as well as the outer one. Compare this partial profile to the total one (Fig. 7, top left). Some further examples of subpulses peaking in the profile centre were also found at 1400 MHz, and the partial profile of 87 such pulses (not shown) shows a strong triple form, but the three features are not well enough resolved to measure the width of the central one.

Pulsar B1133+16 is one of the brightest pulsars in the northern sky, and its geometry has been studied by many groups. Its relatively shallow PPA traverse implies a larger sight-line impact angle of 4:1, thus its narrow ‘intrapulse’ bridge despite its primarily outer cone emission (ET VIa; ET VIb). Similarly, the expected polar cap diameter is 2:2, which viewed at an α of 46° implies a core width of some 3° – agreeing decently with the feature forms in Figs 7 and 8.

4 SUMMARY AND DISCUSSION

Individual pulse observations of the ‘classic’ conal double pulsars B0525+21, B0301+19 and B1133+16 were investigated in detail

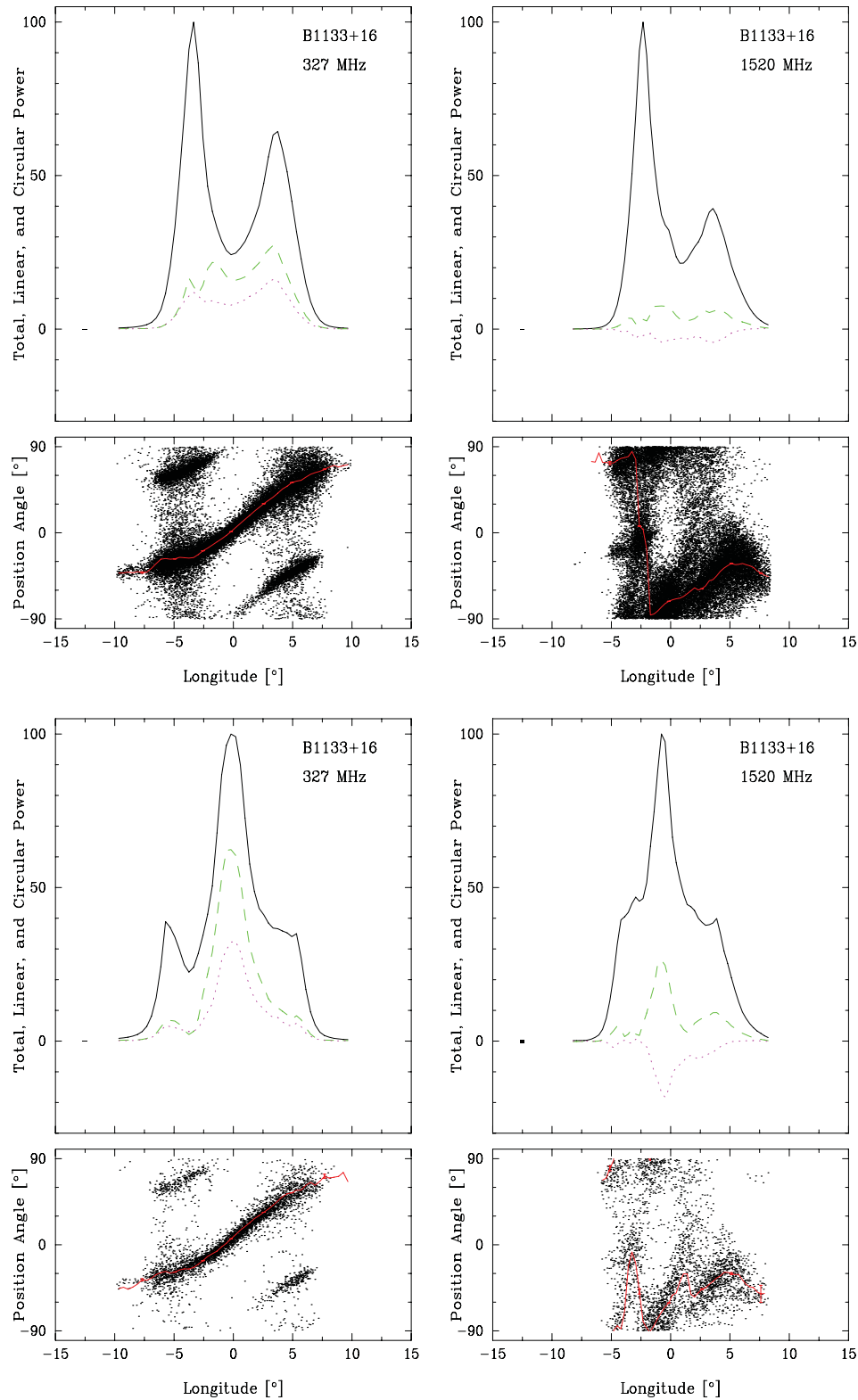


Figure 7. Total average (upper) and suppressed outer conal (lower) profiles of pulsar B1133+16 at both 327 MHz (left) and 1400 MHz (right) as in Fig. 3. At the lower frequency the suppression level was 0.2 (I) and the intrapulse search region $\pm 1^{\circ}.57$ wide, such that 1342 and 180 qualifying pulses were averaged, respectively. At 1400 MHz the suppression level was 0.3 (I) and the search region width was $\pm 1^{\circ}.4$, so 1010 and 120 pulses were averaged. Both lower plots show significant intrapulse emission, and as with B0301+19 above the central region is so narrow that some conal ‘spillover’ is unavoidable.

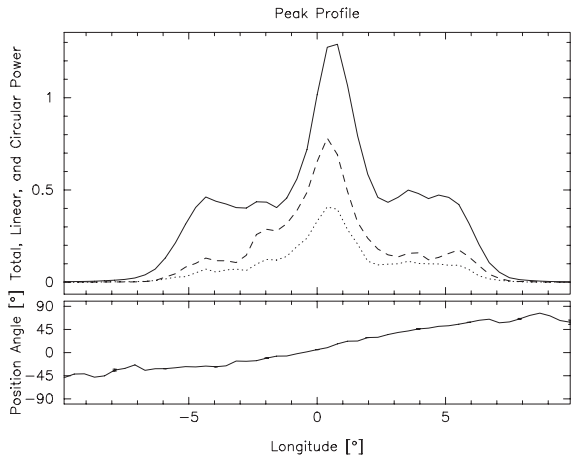


Figure 8. Pulsar B1133+16 at 327 MHz: the 26-pulse partial profile shows the aggregate of pulses that have significant peaks in the ‘intrapulse’ region of the star’s profile.

using several different techniques in an effort to understand the character of their central ‘intrapulse’ emission. Several preliminary studies had suggested weak core emission might be detectable in this region, motivating this larger effort. A summary of the results is as follows.

(i) Populations of individual subpulses were identified in the central regions of these ‘classic’ conal double pulsars that are difficult to regard as having a conal origin.

(ii) Each star exhibited subpulses peaking in the central region during intervals when the surrounding conal emission was weak or absent.

(iii) In each case the longitude distribution of this central population of subpulses was narrower than the width of the ‘intrapulse’ region examined.

(iv) ‘Core flares’ lasting for up to 10 periods or so were positively identified in pulsar B0525+21 at 327 MHz; however, in all other cases bright central subpulses persisted for much shorter intervals.

(v) The aggregate widths of features comprised of this central emission agree well with the expected polar cap widths of core components.

(vi) Aggregations of the central subpulses were more highly circularly polarized than the surrounding conal emission, but no anti-symmetric circular was observed.

(vii) Central subpulses are more irregular than weak: such emission is most readily identifiable when the surrounding conal emission is weak; however, the partial profiles show that its intensity is then comparable to the residual conal emission.

These populations of central subpulses, detected in pulsars B0301+19, B0525+21 and B1133+16 at both 1400 and 327 MHz, exhibit aggregate characteristics very similar to those of core components. We also examined B0751+32, B2044+15 and B1924+14, and these other stars with ‘classic’ conal double profiles exhibited

similar properties, but their smaller S/N values made it difficult to assemble clear enough evidence to present here.

Overall, this central emission so closely resembles core emission both dynamically and geometrically that we believe it very difficult to understand it otherwise. Indeed, the idea that core emission might be found in the ‘intrapulse’ bridge regions of conal double pulsars is not new; these regions are so difficult to understand in conal terms that one of us speculated upon it previously in ET I. Similarly, partial profiles of lower intensity pulses often seem to provide clearer or more complete indications about the full structure of a pulsar’s profile (see e.g. Mitra, Rankin & Gupta 2007; Mitra & Rankin 2011). What is new here is a thorough single-pulse-based analysis of the ‘bridge’ emission in pulsars with only an outer conal pair of components, including a new method to suppress the latter. That the main result is detection of signatures of core and inner cone emission should not be any shock, because the overwhelming evidence is that the fundamental beam structure of most radio pulsars is comprised of concentric double conal and core radiation beams.

ACKNOWLEDGMENTS

We are pleased to acknowledge Dipanjan Mitra and Geoff Wright for their critical readings of the manuscript and Jeffrey Herfindal for assistance with aspects of the analysis. SAEY thanks the UVM College of Arts and Sciences for the APLE Summer Fellowship that allowed her to finish this work. Portions of this work were carried out with support from US National Science Foundation Grants AST 99-87654 and 08-07691. The Arecibo Observatory is operated by SRI International under a cooperative agreement with the US NSF (AST-1100968), and in alliance with Ana G. Méndez-Universidad Metropolitana, and the Universities Space Research Association. This work used the NASA ADS system.

REFERENCES

- Backer D. C., 1975, *ApJ*, 209, 895
 Hankins T. H., Rankin J. M., 2010, *AJ*, 139, 168
 Herfindal J. L., Rankin J. M., 2007, *MNRAS*, 380, 430
 Herfindal J. L., Rankin J. M., 2009, *MNRAS*, 393, 1391
 Komesaroff M. M., 1970, *Nat*, 225, 612
 Lyne A. G., Manchester R. N., 1988, *MNRAS*, 234, 477
 Mitra D., Rankin J. M., 2002, *ApJ*, 557, 322 (ET VII)
 Mitra D., Rankin J. M., 2011, *ApJ*, 727, 92
 Mitra D., Rankin J. M., Gupta Y., 2007, *MNRAS*, 379, 932
 Radhakrishnan V., Cooke D. J., 1969, *Astrophys. Lett.*, 3, 225
 Rankin J. M., 1983, *ApJ*, 274, 333 (ET I)
 Rankin J. M., 1986, *ApJ*, 301, 901
 Rankin J. M., 1990, *ApJ*, 352, 247 (ET IV)
 Rankin J. M., 1993a, *ApJ*, 405, 285 (ET VIa)
 Rankin J. M., 1993b, *ApJS*, 85, 145 (ET VIb)
 Rankin J. M., Ramachandran R., 2003, *ApJ*, 590, 411
 Ruderman M., Sutherland P., 1975, *ApJ*, 196, 51

This paper has been typeset from a \LaTeX file prepared by the author.